MR imaging contrast enhancement and segmentation using fuzzy clustering

A. Djerouni, H. Hamada, and N. Berrached

Intelligent Systems Research Laboratory, LARESI
University of Sciences and Technology of Oran, P.O. Box 1505 El M'naouar, Oran, Algeria

Abstract

One of the most important stages in medical image analysis is objects segmentation. Segmentation results can be heavily affected by image quality. Medical images usually present undesired properties such as low signal-to-noise (SNR) and contrast-to-noise (CNR) ratios, as well as multiple and discontinuous edges. This explains why image enhancement takes an important role in the segmentation and analysis process result. Our aim in this paper is to present a method for medical image segmentation based on the fuzzy c-means (FCM) algorithm preceded by a local image contrast enhancement procedure. This method can be considered as a kind of convolution filter but presents the originality of the adaptive found of convolution mask coefficients. The grey level distribution of pixels in the neighborhood of the current pixel is considered as $1/r^2$ distribution, which was deduced from the Newtonian model, where r is a hybrid distance which involves the spatial information and the luminance one. Finally, some results are presented in order to show the computational performance of this approach.

Keywords: *Image enhancement, Image segmentation, Magnetic resonance imaging, Fuzzy clustering.*

1. Introduction

Medical imaging techniques such as, Magnetic Resonance Imaging (MRI), Computed Tomography (CT) or Ultrasound Imaging (USI) have introduced a formidably powerful tool in medicine by providing detailed images of internal organs. Quantitative information, like organ size and shape, can be extracted from these images in order to support activities such as disease diagnosis, monitoring and surgical planning (Grossman and McGowan, 1998). However, in order to accomplish this, it is first necessary to identify the different tissues and anatomical structures being involved (Pham et al, 2000). Medical images usually present characteristics such as low SNR and CNR ratios, due to various types of artifacts introduced during the acquisition process (imperfection of experimental process, such as magnetic field inhomogeneities for MRI external RF interference). High SNR is always desirable because of its benefit for image segmentation, visibility of the vessels or enhancement of larger structures. Image enhancement is a very powerful tool to improve the quality of a degraded image. In image processing, a high SNR is also required because most of the image segmentation algorithms are very sensitive to noise. Different techniques have been studied to improve the SNR of a degraded image.

Basically there are two classes of approaches to improve SNR. One is changing the acquisition methods or improving relative equipments, such as averaging multiple acquisitions, scanning with large voxels, or upgrading hardware. Another one is to post process image data after acquisition using filtering methods. Ideal result of filtering is to remove noise while preserving the boundary and the detail structure information. The conventional linear spatial smoothing method usually averages the brightness of the neighbors of a pixel and takes the result as the smoothed value of this pixel, (also called low-pass filtering; isotropic diffusion). This method downgrades noise, but also blurs edges and damages fine structures. This effect can be reduced by using non-linear filters. A smoothing method proposed by (Perona and Malik, 1990) using anisotropic diffusion model has been shown to possibly overcome the drawbacks of conventional linear spatial smoothing method. In this paper we present a method for detection of multiple sclerosis lesions in multispectral MR using the FCM algorithm which is an unsupervised pixel classification technique based on iterative approximation to local minima of global objective function preceded by a local image contrast enhancement procedure called the Newtonian Operator (NO) inspired from (Perona and Malik, 1990) and the Newton's law of gravitation.

2. Background

2.1 Multiple sclerosis data

Multiple sclerosis is a progressive disease with lesions evolving over time. Lesions appear in the central nervous system: encephalon, especially the white matter, spinal cord and optic nerves. MRI scans make possible the diagnosis confirmation at the beginning of multiple sclerosis. Moreover, MRI scans also make possible to follow-up a patient with multiple sclerosis evolving over time. The need of brain MRI as a more specific and more sensitive outcome measure in monitoring multiple sclerosis patients and in testing new therapies is generally accepted. The choice of MRI techniques for multiple sclerosis lesions (MSL) is not defined as an evidence for physicians. Quantitative measurements, such as the surface or intensity variation of lesions or segmentation of evolving lesions, are important. To this end, image segmentation techniques are required. This operation consists in partionning the MRI image into anatomic tissues, fluids and other structures. This suggests the importance of adequate image pre-processing techniques before image interpretations. To study multiple sclerosis lesions in time series, it is possible to threshold or to study the image intensity, to segment lesions independently at each time point. We can also subtract two successive images to find intensity changes. Different methods have been proposed for automated a nd semi automated detection of MSL with varying degrees of automation and operator interaction approches. The geometry-driven methods use the overall shape of an object to separate it from its surroundings in the image (Lötjönen et al, 1999; Zeng et al, 1999; Gonzalez et al, 2000; Xu et al, 2000; McInerney and Terzopoulos, 1996). The intensity-driven methods fit appropriate intensity models to the data, often explicitly taking imaging artefacts into account, such as the partial volume effect (Nagao and Matsuyama, 1979; Santago and Gage, 1993; Laidlaw et al, 1998) and the intensity inhomogeneity present in MR images (Wells, 1996, Held et al, 1997; Guillemaud and Brady, 1997). These methods can be categorized into classical, statistical, fuzzy and neural network. An exhaustive review of these classification methods is beyond the scope of this paper but we refer the interested reader to (Pal, R. and Pal, S. K., 1993; Suri et al, 2002; Pham et al, 2000).

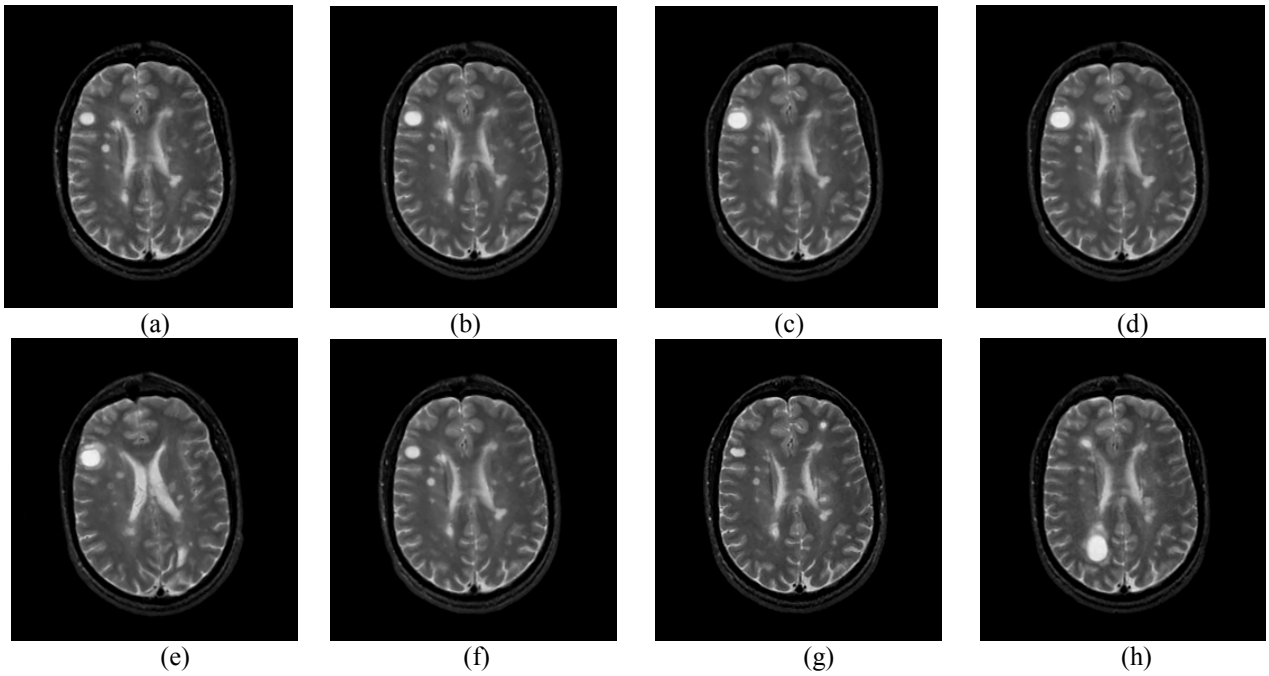

Fig.1. MS lesion evolution over one year's time. (a) The large round white spot in the right frontal region is a relatively new lesion. It enlarges very rapidly over the next weeks. (b) (c) (d) With time, the lesion enlarges, there is a "halo" of white (high) signal which surrounds the lesion). (c) (d) (e) This probably represents the edema which forms in reaction to the acute damage. (f) (g) At the end, the lesion has nearly disappeared, with another lesions appearing. There is a large variety of lesion sizes, ranging from a tiny spot, to the huge lesion.

2.2 Method

The method used for lesion segmentation is shown in (Fig. 2).

MRI brain images

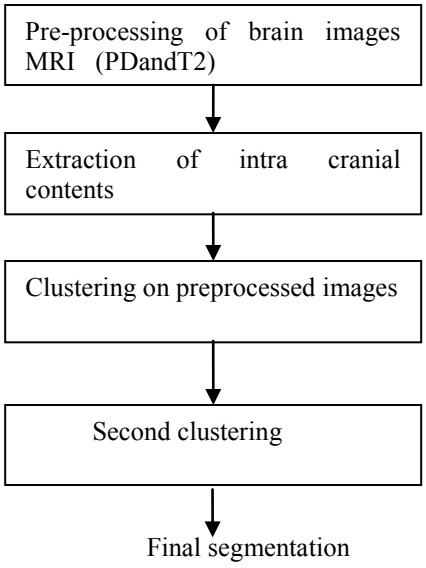

Fig.2. Block diagram illustrating the MS lesions segmentation

At first, the images are preprocessed to increase the contrast between CSF and lesions. The segmentation field is narrowed by extracting the intracranial contents of the brain using a binary mask. Then the images are segmented using the Fuzzy c-means (FCM) algorithm.

2.3 Preprocessing of images

Image enhancement process increases the relative intensity level of the wanted structures in the image and improves their detection sensitivity. In this work, a new method for filtering MR images with spatially varying noise levels is presented.

This method can be considered as a member of convolution filters set but presents the originality of the adaptive found of convolution mask coefficients. The grey level distribution of pixels in the neighborhood of the current pixel is considered as $1/r^2$ distribution, which was deduced from the Newtonian model, where r is a hybrid distance which involves the spatial information and the luminance one. A neighborhood operation takes the values of pixels in the neighborhood of a point, performs some operations with them, and writes the results back on to the point. The grey level intensities inside the neighborhood window, can be calculated using the following formula: (Ouremchi et al, 2000)

$$\vec{F} = G\frac{m_1 m_2}{r^2}\vec{u} \qquad (1)$$

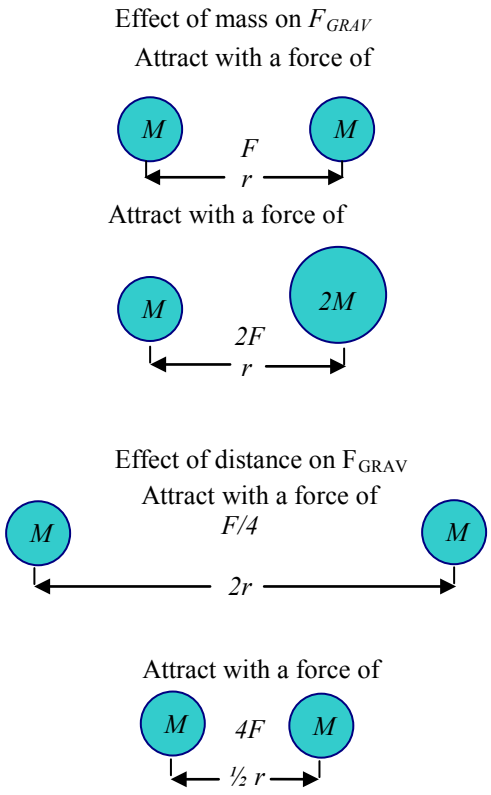

Fig.3. Illustration of the proportionalities expressed by Newton's universal law of gravitation

F is the magnitude of the gravitational force between the two point masses,

- G is the gravitational constant,
- m_1 is the mass of the first point mass,
- m_2 is the mass of the second point mass,
- r is the distance between the two point masses.

If we consider the grey level intensities in a neighborhood window as information particles, there is an interaction force among these particles. The proportionally expressed by Newton's universal law of gravitation is represented graphically by Fig. 3. We can see that the force of gravity is proportional to the product of the two masses and inversely proportional to the square of the distance of separation.

In the proposed method, m_1 and m_2 represents the values of pixels. G the gravitational constant is replaced by the constant k.

$$\vec{F_i} = k\frac{g_i g_j}{r_{ij}^2}\vec{u} \qquad (2)$$

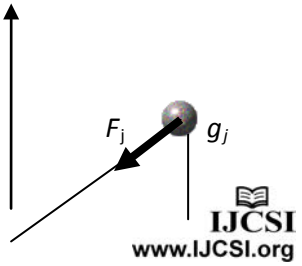

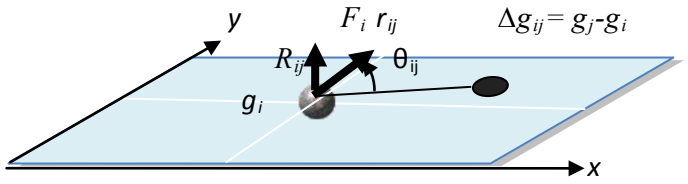

Fig.4 3D Enhancing representation

$$r_{ij} = d_{ij}^2 + \Delta g_{ij}^2 \quad (3)$$

Where r_{ij} is the hybrid distance between the centers of the two pixels neighbors « i », « j ». $(x_i, y_i), (x_j, y_j)$ are the spatial coordinates respectively of the pixels i, j in the x, y directions and g at (x, y) is related to the brightness of the image at that point. $g(x_i, y_i)$ is the characteristic feature function (e.g. gray level) with

$$d_{ij}^2 = (x_i - x_j)^2 + (y_i - y_j)^2 \quad (4)$$

$$\Delta g_{ij} = g_j - g_i \quad (5)$$

The parameter k is a constant positive. If we consider the luminance information, the projection of the interactions force in the direction (g_i, g) is given by the following equation

$$\overrightarrow{R_{ij}} = k \sum_j \frac{g_i g_j}{r_{ij}^2} \sin\theta_{ij} \overrightarrow{u_j} \quad (6)$$

$$\sin\theta_{ij} = \frac{\Delta g_{ij}}{r_{ij}} \quad (7)$$

We can write R_{ij} as

$$R_{ij} = k \sum_j \frac{g_i g_j \Delta g_{ij}}{\left(\Delta g_{ij}^2 + d_{ij}^2\right)^{3/2}} \quad (8)$$

or also as

$$R_{ij} = g_i \Gamma \quad (9)$$

where

$$\Gamma = k \sum_j \frac{g_j \Delta g_{ij}}{\left(\Delta g_{ij}^2 + d_{ij}^2\right)^{3/2}} \quad (10)$$

which is the field of the grey levels g_j of the pixel «*j*» neighbor of the central pixel« *i*» with a grey level g_i. The grey level varies according to the second law of Newton,

$$g(t) = g_0 + \frac{1}{2}\Gamma t^2 \quad (11)$$

where g_0 is the grey level value at $t=o$ and $g(t)$ is the grey level value at the instant t .

The central pixel «*i*» with the grey level g_0 at $t=o$ becomes $g_i(t)$ at the instant t. Its value is given by the equation

$$g_i(t) = g_0 + \frac{1}{2} k \left(\sum_j \frac{g_j \Delta g_{ij}}{\left(\Delta g_{ij}^2 + d_{ij}^2\right)^{3/2}} \right) t^2 \quad (12)$$

The variation of $g_i(t)$ is a parabola, the grey level of the pixel «*i*» can increase if $\Delta g_{ij} > 0$, decrease if $\Delta g_{ij} < 0$ or stay unchanged if $\Delta g_{ij} = 0$. We adapt this equation for enhancing the contrast by temporal sampling and fixing rate. The processes could be iterative. That is,

$$g_i(t+1) = g_i(t) + \frac{1}{2} k \sum_j \frac{g_j \Delta g_{ij}}{\left(\Delta g_{ij}^2 + d_{ij}^2\right)^{3/2}} \quad (13)$$

$$g_i(t+1) = g_i(t) + \frac{1}{2} k S_{ij} \quad (14)$$

$$S_{ij} = \sum_j \frac{g_j \Delta g_{ij}}{\left(\Delta g_{ij}^2 + d_{ij}^2\right)^{3/2}} \quad (15)$$

S_{ij} could be a gradient or Laplacian operator similar to that proposed by (Rosenfeld and Kak, 2002). A much more successful application of the Laplacian was proposed by (Marr and Hildreth, 1980). This approach first smoothes the image by convolving it with a two dimensional Gaussian function of a given standard deviation σ defined by

$$h(x, y) = \frac{1}{\sqrt{2\pi\sigma^2}} e^{-\frac{x^2+y^2}{2\sigma^2}} \quad (16)$$

The standard deviation σ is proportional to the size of the neighbourhood on which the filter operates.

The operator possesses useful property: the evaluation of the Laplacian and the convolution commute

$$\nabla(f(x, y) * h(x, y, \sigma)) = f(x, y) * \nabla h(x, y) \quad (17)$$

f(x,y) represents the image intensity at a point *(x, y)*.

If we examine the expression of S_{ij} obtained by the proposed method, the distribution *h(.)* is in "*1/r*" and is given by

$$h(\Delta f_{ij}) = \frac{1}{\left(\Delta f_{ij}^2 + d_{ij}^2\right)^{1/2}} \quad (18)$$

We see that it corresponds to (17)

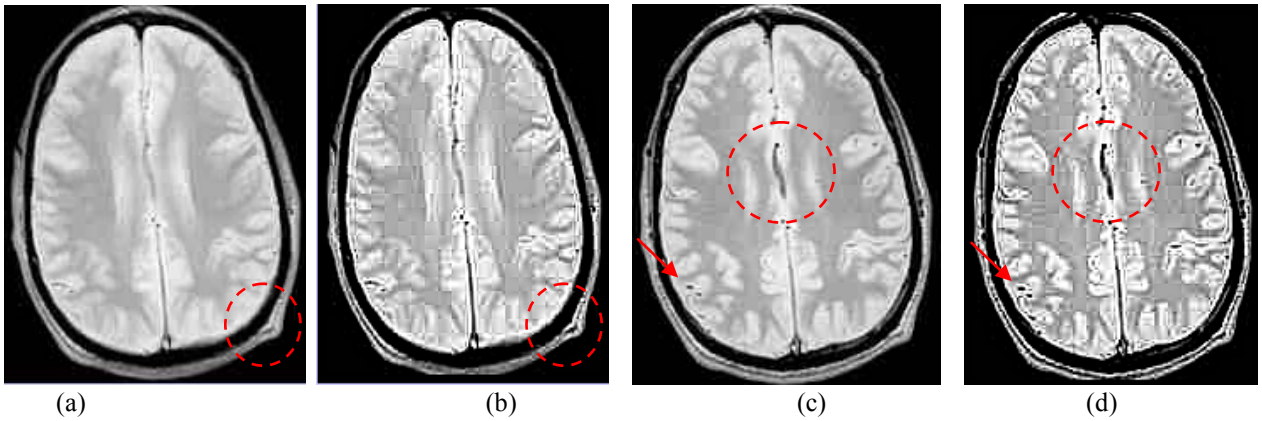

Fig.5. Contrast enhancement preprocessing (a) Axial slice of original PD weighted image with a resolution of 3mm; (b) the enhanced image with the proposed method , the Newtonian operator; (c) Axial slice of original PD weighted image with resolution of 2mm (d) the enhanced image with the proposed method.

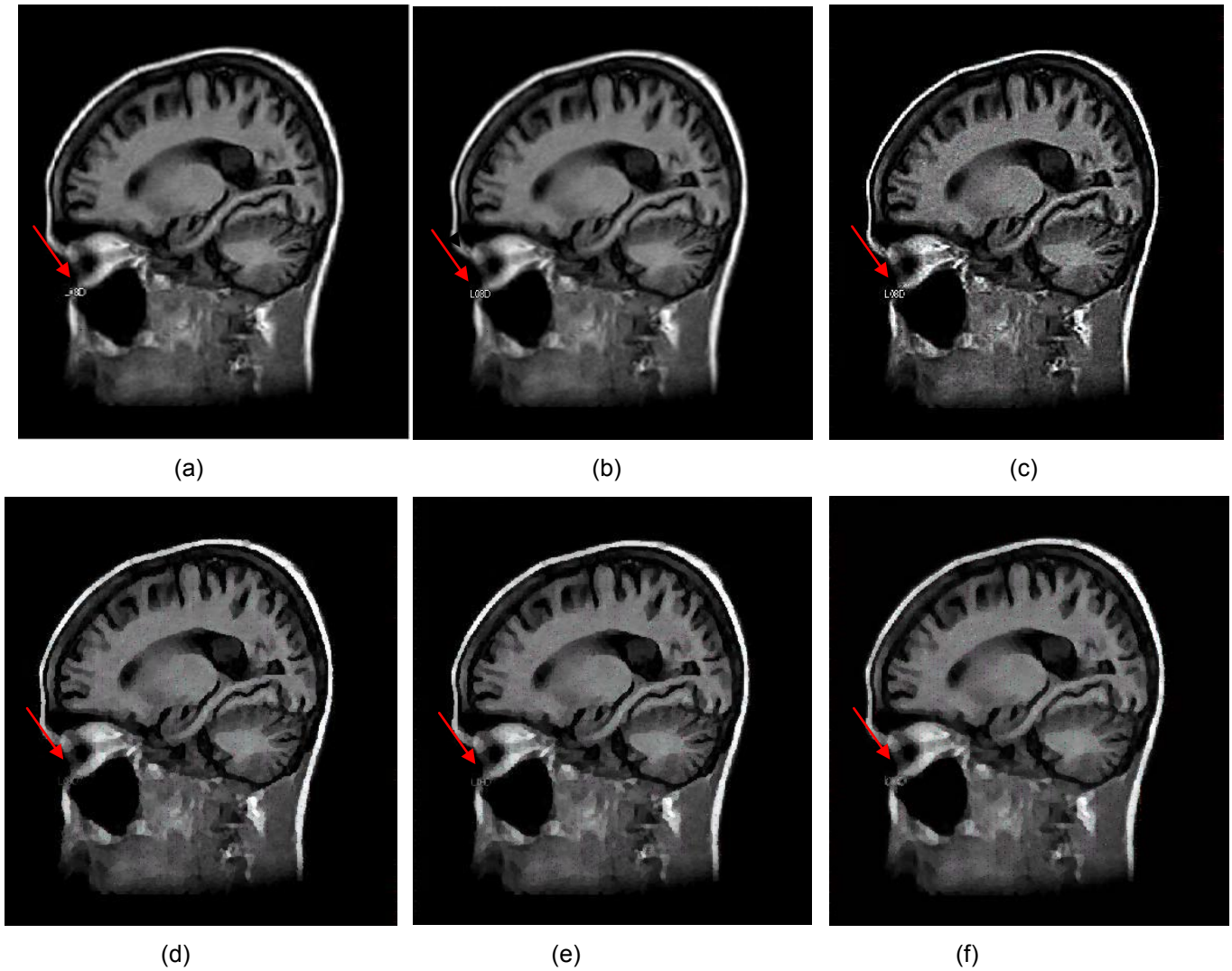

Fig.6. Results from the proposed method (Newtonian operator) contrast enhancement preprocessing compared to (a) Sagittal slice of original T2 weighted image; (b), (c) the enhanced image with the proposed method(k=0.3)and(k=1); (d) Result from Nagao filter; (e) Result from Kuwahara filter; (f) Result from Tomita/Tsuji filter

2.4 Fuzzy segmentation method

The goal of traditional clustering is to assign each data point to one cluster. In contrast, in fuzzy clustering, the data points can belong to more than one cluster. The

membership of a point is thus shared among various clusters. This creates the concept of fuzzy boundaries which differs from the traditional concept of well-defined boundaries. In this section, we give a b rief overview of Fuzzy C-Means algorithm (FCM) which is one of the most widely used in fuzzy clustering. This technique was originally introduced by (J. Bezdek in 1981).

Let $X = \{x_1, \ldots\ldots x_n\}$ be a finite data set and $c \geq 2$ an integer and let $R^{c \times n}$ denotes the set of all real $c \times n$ matrices. A fuzzy c-partition of X is represented by a m atrix $U = [\mu_{ik}] \in R^{c \times n}$ with respect to some given criterion.

$$\mu_{ik} \in [0,1] \quad 1 \leq i \leq c; \quad 1 \leq k \leq n$$

$$\sum_{i=1}^{c} \mu_{ik} = 1; \quad 1 \leq k \leq n$$

$$\sum_{k=1}^{n} \mu_{ik} > 0; 1 \leq i \leq c \qquad (19)$$

U can be used to describe the cluster structure of X by interpreting μ_{ik} as the degree of membership of x_k to cluster «i». FCM is formulated as the minimization of the following objective function:

$$J_m(U, V: X) = \sum_{k=1}^{n} \sum_{i=1}^{c} (\mu_{ik})^m \|x_k - v_i\|_A^2 \qquad (20)$$

where $m \in [1 \ +\infty]$ is a weighting exponent called the fuzzifier, $V = (v_1, v_2, \ldots.v_c)$ is the vector of the cluster centers, $\|x\|_A = \sqrt{x^T A x}$ is any product norm where A is any positive definite matrix .

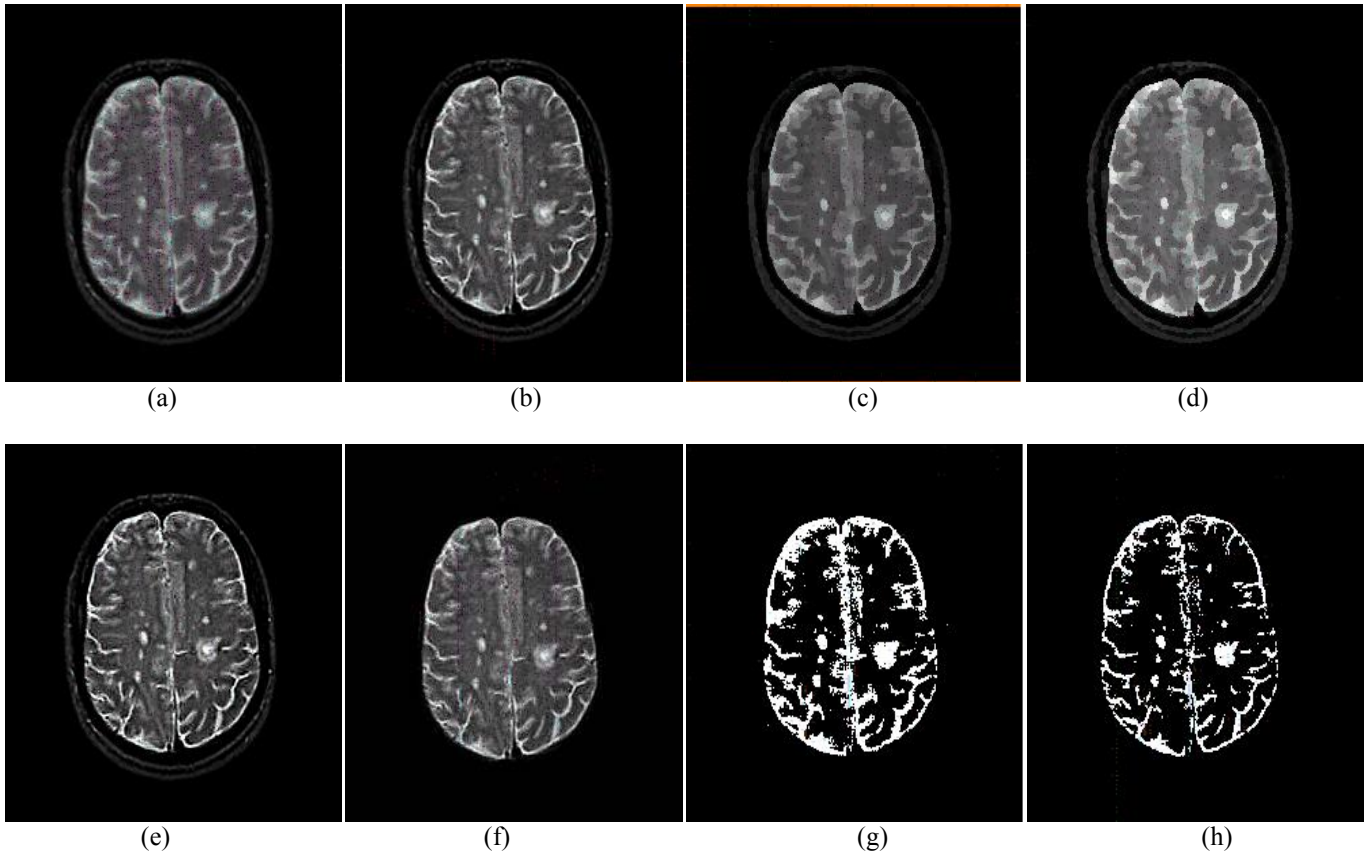

(a) (b) (c) (d)

(e) (f) (g) (h)

Fig.7. (a) Axial slice of original T2 weighted image; (b) result of the proposed method (Newtonian operator) k=0.5; (c) Nagao filter; (d) Kuwahara filter; (e) result of the proposed method (Newtonian operator) k=1; (f) extraction of the intracranial contents from the enhanced image (b) by the Newtonian operator; (g) Fuzzy segmentation of the original image; (h) Fuzzy segmentation of the preprocessed image by the Newtonian operator.

FCM Theorem (Bezdek, 1981).

(U, V) may minimize J_m only if

$$\mu_{ik} = \left[\sum_{j=1}^{c} \left(\frac{\|x_k - v_i\|_A}{\|x_k - v_j\|_A} \right)^{\frac{2}{m-1}} \right]^{-1} \qquad (21)$$

$$v_i = \frac{\sum_{k=1}^{n} (\mu_{ik})^m . x_k}{\sum_{k=1}^{n} (\mu_{ik})^m} \qquad (22)$$

The FCM consists of iterations alternating between Eqs (21) and (22) from an arbitrary partition till the iteration process converges. The final stage of the FCM clustering is to interpret the membership function, by classifying a v oxel to the cluster with the largest membership.

The following algorithm uses an histogram based gray-level fuzzification. The FCM only operates on the histogram and consequently is faster than the conventional version (Bezdek, 1981) which processes the whole data set. The algorithm is outlined in the following steps:

⟨ **FCM1**⟩ Fix the number of clusters *c, 2≤c≤L* where *L* is the number of grey levels and the threshold value ε

⟨**FCM2**⟩ Find the number of occurrences *H (l)* of the level *l=0, 1,..., L-1*

⟨**FCM3**⟩ initialise the membership degrees such that $\sum_{I=1}^{C} \mu_{il} = 1; l \ldots L-1$

⟨**FCM4**⟩ Compute the new centroids

$$v_i = \frac{\sum_{l=0}^{L-1}(\mu_{il})^m . H(l) . l}{\sum_{l=0}^{L-1}(\mu_{ik})^m . H(l)}$$

⟨**FCM5**⟩ update the memberships μ_{il} *to* $\tilde{\mu}_{il}$

$$\widetilde{\mu_{il}} = \left[\sum_{j=1}^{c}\left(\frac{\|l-v_i\|}{\|l-v_j\|}\right)^{\frac{2}{m-1}}\right]^{-1}$$

⟨**FCM6**⟩

Compute $U^{(l+1)}$

$E = \|U^{l+1} - U^{l}\|$

If

$E > \varepsilon$

$\mu_{il} \leftarrow \tilde{\mu}_{il}$

Go to ⟨**FCM4**⟩

⟨**FCM7**⟩ Defuzzification process

3. Results

In this section we present some results on real MRI brain images using the method introduced to enhance tissues and to segment MS lesions. Quantification based on T2 and PD weighted image is considered to be the primary image based marker of MS lesions (Udupa et al, 1997). These two images show the lesions as hyper signal regions. In (Fig. 1) an example of axial slices of T2 weighted and in (Fig. 5) axial slices of PD weighed images are shown. In patient with MS lesions (Fig. 1), the lesions appear as brighter objects. The preprocessing result is illustrated in (Fig 5), (Fig. 6), and (Fig.7). One may note that the MS lesions in T2 weighted images are more visible (Fig. 7e). Shown in (Fig 5a), (Fig 5c), we note also the effect of the resolution in PD weighted images with respectively a 3mm resolution and with a 2mm resolution. We clearly see that the separability between the tissues is increased. The intracranial contents (Fig. 7f) are extracted using a binary mask which eliminates the generated noise outside the brain space and accelerates the segmentation process. The fuzzy segmentation is illustrated in (Fig.7h). This segmentation conserves all regions of interest and undesirable structures are reduced. The major criterion for performance evaluation is whether the method can indicate interesting or important regions in the image. A segmentation method can, therefore, be declared successful if it can identify the most important lesions. The final result is obtained using anatomical knowledge. Different window sizes ranging from 5x5 to 25x25 (Table 2) are tested to locally enhance the slices. There is no method to automatically find the adequate window size. We have compared the proposed method with different algorithms known in the literature (Kuwahara, 1976; Tomita and S. Tsuji, 1997; Nagao and Matsuyama, 1979) to show its performance. The Kuwahara filter is an edge-preserving filter based on local area flattening. The Kuwahara filter removes detail in high-contrast regions while protecting shape boundaries in low-contrast regions. Therefore, it helps to maintain a roughly uniform level of abstraction across the image while providing an overall painting-style look. The Kuwahara filter is unstable in the presence of noise. Several extensions and modifications have been proposed (Papari et al, 2007) to improve the original Kuwahara filter. (Tomita and Tsuji, 1997) proposed a variance-based filter. They obtained the mean and variance in five *(2m+ 1) x (2m+ 1)* windows, which placed the pixel being filtered at the four corners or the center, and defined the filter output to be the mean of that window which had the smallest variance. This filter is based on the idea that each pixel belongs to one of a number of internally homogeneous regions, and that one of the five windows will lies completely or mainly within the region to which the pixel belongs. That window should have minimum variance, and its mean is then an estimate of the mean intensity for the region. The filter is readily extended to more than five windows. The Nagao filter computes mean and variance for 9 different operator masks. The central pixel is assigned the average value of the sub window with the smallest variance.

In denoising or enhancing applications, the performance is often measured using quantitative performance measures such as peak signal-to-noise ratio (PSNR), SNR as well as in terms of visual quality of the images. The PSNR is more easily defined via the mean squared error (MSE) which for two *mxn* monochrome images *I* and $\hat{I}$ (where one of the images is considered a noisy approximation of the other) is defined as:

$$MSE = \frac{1}{m \times n}\sum_{i=0}^{m-1}\sum_{j=0}^{n-1}\left[I(i,j) - \left(\hat{I}\,(i,j)\right)\right]^2 \qquad (23)$$

The PSNR can be defined as follows:

$$PSNR = 10.log_{10}\left(\frac{MAX_I^2}{MSE}\right) \quad (24)$$

MAX_I is the maximum possible pixel value of the image. When the pixels are represented using 8 bits/ sample, this gives 255. More generally, when samples are represented with B bits per sample, MAX_I is 2^B-1.

3.1 PSNR Comparisons

We have tested the various denoising methods for a set of 8-bit grayscale images with different sizes (512 x512), (256 x256) noise-free and corrupted by simulated additive noise at different power levels, which corresponds to different PSNR decibel values. The denoising process has been performed over different noise realizations. The PSNR values for the three compared methods for different levels of noise show the efficiency of the Newtonian Operator (NO). Table I summarizes some of the experimental results.

Many of the current techniques assume the noise model to be Gaussian. In reality, this assumption may not always hold true due to the varied nature and sources of noise. An ideal denoising procedure requires a priori knowledge of the noise, whereas a practical procedure may not have the required information about the variance of the noise or the noise model. Thus, most of the algorithms assume known variance of the noise and the noise model to compare the performance with different algorithms. MRI noise is known to follow a Rician density (Hákon Gudbjartsson et al, 1995), which can be fairly approximated by a Gaussian distribution. Noise with different variance values is added in the natural images to test the performance of the algorithm.

3.2 Visual Quality

There is no consensual objective way to judge the visual quality of a denoised image. Two important criteria are widely used: the visibility of processing artifacts and the conservation of image edges. The image quality and diagnostic value of MRI of the human brain are primarily determined by the spatial resolution, SNR, and tissue contrast. Because these entities are interdependent, their simultaneous improvement is not simple or straightforward. For example, reduction of the image voxel volume leads to a proportional decrease in SNR.

Table 1. Comparison of the Proposed Method Newtonian Operator (NO) with the Kuwahara, Nagao, Tomita Filters with Different Image Sizes and Different Values of the Parameter k

	image (512X512)			image (256X256)		
Method	PSNR(dB)			PSNR(dB)		
K	1	0.8	0.5	1	0.8	0.5
Newtonian Operator	30.40	31.99	34.83	24.44	26.37	30.42
Kuwahara Filter			26.94			22.63
Tomita filter			31.04			28.39
Nagao filter			30.33			26.91

Table 2. Influence of k on the output of the proposed operator .PSNR values (dB) obtained for different windows sizes and for different k.Test image (256x256) and output of the proposed operator for k = 1; 0.5; 0.4, 0.2, 0.1 respectively.

	k=1	K=0.5	K=0.4	K=0.2	K=0.1
5x5	24.99	29.25	30.22	31.98	32.56
7x7	24.95	29.20	30.17	31.92	32.50
25x25	22.87	25.74	26.25	27.06	27.28

Table 3. Computation Time Of Various Denoising Techniques.

Method	Unit of Time[s] image (512x512)			image (256x256)		
K	1	0.8	0.5	1	0.8	0.5
Newtonian Operator	36.77	38.70	39.35	11.76	19.56	16.08
Kuwahara Filter			25.46			6.20

Nagao Filter	39.81	10.19
Tomita/Tsuji Filter	33.00	8.40

Furthermore, excellent tissue contrast between gray matter (GM) and white matter (WM), the two main tissue components of the human brain, can be readily achieved by sensitizing the MRI acquisition technique to tissue relaxation times T1 and T2, but not without substantial loss in SNR.

3.3. Computation Time

It is also interesting to evaluate the various denoising methods from a practical point of view: the computation time. Due to the complexity of the calculations, the proposed algorithm needs more computation time than the algorithms used for comparaison (table 3). In the presented example a window of size 7x7 pixels has been used.

4. Conclusion

We have presented a n ovel enhancing method for medical images, namely the Newtonian operator (NO). The method integrates the spatial information and the luminance one to preprocess medical images. In order to evaluate the performance of the Newtonian operator (NO), we have conducted several experiments on 2D medical images. The experimental results have shown that our novel method is capable of producing greater noise reduction and enhancing the images without over-smoothing the edges, as compared to other edge-preserving noise reduction methods. Additionally, the application of the post processing tasks — segmentation and feature extraction (lesions detection) — on the filtered images has demonstrated that the method is an adequate pre-processing technique for improving the quality of segmentation and facilitating the feature extraction. More sophisticated post processing is envisaged in order to measure precisely the lesion area. Our current research aims to quantify the sensitivity of the algorithm to the parameter *k* as well as the effect of neighboring. We expect to make the classification more robust to noise and inhomogeneities. We shall pay more attention to visual effect. We will mainly focus on how to make the algorithm faster.

References

[1] J.C. Bezdek, "Pattern recognition with fuzzy objective function algorithms ," Plenum Press New York, 1981.

[2] H. S. Choi, D. R. Haynor, and Y. M. Kim, "Partial volume tissue classification of multichannel magnetic resonance images — a mixel model," IEEE Transactions on Medical Imaging, vol. 10, no. 3, pp. 395–407, 1991.

[3] L.P. Clarke, R. P. Velthuizen, M. A. Camacho, J. J. Heine, M.Vaidyanathan, L. O. Hall, R. W. Thatcher, and M. L. Silbiger, "MRI segmentation: Methods and applications", Magn. Reson. Imag., vol. 13,no. 3, pp. 343–368, 1995.

[4] M. A. González Ballester, A. Zisserman, and M. Brady, "Segmentation and measurement of brain structures in MRI including confidence bounds," Medical Image Analysis, vol.4, pp. 189–200, 2000.

[5] R.I. Grossman, and J.C. McGowan, "Perspectives on multiple sclerosis," AJNR, vol.19, pp. 1251–1265, 1998.

[6] R. Guillemaud, and M. Brady, "Estimating the bias field of MR images," IEEE Transactions on Medical Imaging, vol. 16, no. 3, pp. 238–251, 1997.

[7] H. Gudbjartsson, and S. Patz, "The Rician Distribution of Noisy MRI Data," Magnetic Resonance in Medicine, 34: 910-914, 1995.

[8] K. Held, E. R. Kops, B. J. Krause, W. M. Wells, R. Kikinis, and H-W. Müller Gärtner. "Markov random field segmentation of brain MR images", IEEE Transactions on Medical Imaging, vol. 16, no. 6, pp. 878–886, , 1997.

[9] M. Kuwahara, K. Hachimura, S. Eiho, and K. Kinoshita, "Digital Processing of Biomedical Images", Plenum Press, pp. 187-203, New York, NY, 1976.

[10] J. Lötjönen, P.J. Reissman, I.E. Mangin, and T. Katila," Model extraction from magnetic resonance volume data using the deformable pyramid," Medical Image Analysis, vol. 3, no.4, pp. 387–406, 1999.

[11] D. H. Laidlaw, K. W. Fleischer, and A. H. Barr, "Partial-volume Bayesian classification of material mixtures in MR volume data using voxel histograms," IEEE Transactions on Medical Imaging, vol. 17, no. 1, pp. 74–86, 1998.

[12] D. Marr and E. Hildreth, "Theory of edge detection," Proc. Roy. Soc, London, vol. B207, pp. 187-217. 1980.

[13] T. McInerney and D. Terzopoulos, "Deformable models in medical image analysis: a survey," Medical Image Analysis, vol. 1(2), pp. 91–108, 1996.

[14] M. Nagao and T. Matsuyama, "Edge preserving smoothing," Computer Graphics and Image Processing, vol. 9, pp.374-407, 1979.

[15] R. Ouremchi, , R. Benslimane, and T. Gadi, , "Un opérateur Newtonien pour le rehaussement de contraste,"Traitement du signal. Vol 17-n° 5. 2000.

[16] N. R. Pal and S. K. Pal, "A review on image segmentation techniques," Pattern Recognition, vol. 26, no. 9, pp.1277 - 1294, 1993.

[17] G. Papari, N. Petkov, and P. Campisi. "Artistic Edge and Corner Enhancing Smoothing," IEEE Transactions on Image Processing, vol.16, no.10, pp.2449-2462, 2007.

[18] P. Perona, and J. Malik, "Scale-Space and Edge Detection Using Anisotropic Diffusion," IEEE Transactions on Pattern

Analysis Machine Intelligence, vol. 12, no. 7, pp. 629-639, 1990.
[19] D. L. Pham, C. Xu, and J. L. Prince, "Current Methods in Medical Image Segmentation," Annual Review of Biomedical Engineering, vol. 2 , pp. 315-338, 2000.
[20] A. Rosenfeld and A. C.Kak, "Digital Image Processing,"2nd ed., vol. 1, Academic Press, New York, 1982.
[21] P. Santago and H.G. Gage. "Quantification of MR brain images by mixture density and partial volume modeling," IEEE Transactions on Medical Imaging, Vol. 12,no.3, pp. 566 -574, 1993.
[22] J. S. Suri, S. Singh, and L. Reden, "Computer vision and pattern recognition techniques for 2-D and 3-D MR cerebral cortical segmentation (part I): A state-of-the-art review," Pattern Analysis and Applications, Vol. 5, no. 1, pp. 46–76 2002.
[23] F. Tomita and S. Tsuji, "Extraction of Multiple Regions by Smoothing in Selected Neighborhoods," IEEE. Transaction on Systems, Man and Cybernetics, vol. 7, pp. 107-109, 1977.
[24] J.K. Udupa, L. Wei, S. Samarasekera, Y. Miki, M.A. van Buchem, and R.I. Grossman, "Multiple Sclerosis Lesion Quantification Using Fuzzy-Connectedness Principles," IEEE Transactions Medical Imaging, vol. 16,no..5, pp. 598-609, 1997.
[25] W. M. III Wells, W. E. L. Grimson, R. Kikinis and F. A. Jolesz, Adaptive segmentation of MRI data. IEEE Transactions on Medical Imaging, vol 15, no.4, pp. 429–442, 1996.
[26] C. Xu, D. L. Pham, M. E. Rettmann, D. N. Yu, and J. L. Prince, "Reconstruction of the human cerebral cortex from magnetic resonance images," IEEE Transactions on Medical Imaging, vol. 18, pp. 467–480, 1999.
[27] X. Zeng, L. H. Staib, R. T. Schultz, and J. S. Duncan, "Segmentation and measurement of the cortex from 3D MR images using coupled surfaces propagation," IEEE Transactions on Medical Imaging, vol. 18, no. 10, pp. 927–937, 1999.

Aicha Djerouni received the Magister degree in electrical engineering in 1985 from the University of Sciences and Technology of Oran. Since 2000, she has been a R esearch Assistant at Intelligent Systems Research Laboratory. She currently teaches television at the Electronics Department, Electrical and E lectronics Engineering Faculty, University of Sciences and Technology of Oran. Her main research area focused on biomedical signals and image processing and analysis. She has a strong interest in television and video processing.

Hocine Hamada received the M.S. degree in electronics engineering in 1978 at USTO, the Diplôme d'Etudes Approfondies (DEA) and Docteur-Ingénieur degrees in E.E.A. (Electronique Electrotechnique Automatique) in 1979 and 1982 respectively from the "Université Paul SABATIER -Toulouse ". He is presently with the Intelligent Systems Research Laboratory. His experience is related to t eledetection, pattern recognition, classification, image processing and analysis.

Nasr-Eddine Berrached received the "doctor of engineering degree" in computer sciences from Tokyo Institute of technology in 1992. He is Professor at the University of Sciences and Technology of Oran where he leads since 2000 the Intelligent Systems Research Laboratory. He is coordinator of the Doctoral School in "New Technologies for Information and Communication, Intelligent Systems, and R obotics". He is Expert of the European Union commission for education: Tempus Program and is also member of the standing committee for scientific research and technology development.